Multi-step magnetization of the Ising model on a Shastry–Sutherland lattice: a Monte Carlo simulation

2012 J. Phys.: Condens. Matter 24 386003

(http://iopscience.iop.org/0953-8984/24/38/386003)

J. Phys.: Condens. Matter **24** (2012) 386003 (6pp) doi:10.1088/0953-8984/24/38/386003

Multi-step magnetization of the Ising model on a Shastry–Sutherland lattice: a Monte Carlo simulation

W C Huang[1], L Huo[1], G Tian[1], H R Qian[1], X S Gao[1], M H Qin[1] and J-M Liu[2,3]

[1] Institute for Advanced Materials, South China Academy of Advanced Photonics Engineering, South China Normal University, Guangzhou 510006, People's Republic of China
[2] Laboratory of Solid State Microstructures, Nanjing University, Nanjing 210093, People's Republic of China
[3] International Center for Materials Physics, Chinese Academy of Science, Shenyang 110016, People's Republic of China

E-mail: qinmh@scnu.edu.cn and liujm@nju.edu.cn

Received 24 May 2012, in final form 8 August 2012
Published 28 August 2012
Online at stacks.iop.org/JPhysCM/24/386003

Abstract
The magnetization behaviors and spin configurations of the classical Ising model on a Shastry–Sutherland lattice are investigated using Monte Carlo simulations, in order to understand the fascinating magnetization plateaus observed in TmB_4 and other rare-earth tetraborides. The simulations reproduce the 1/2 magnetization plateau by taking into account the dipole–dipole interaction. In addition, a narrow 2/3 magnetization step at low temperature is predicted in our simulation. The multi-step magnetization can be understood as the consequence of the competitions among the spin-exchange interaction, the dipole–dipole interaction, and the static magnetic energy.

(Some figures may appear in colour only in the online journal)

1. Introduction

Over the past decades, frustrated spin systems in which all local interactions between every spin pair cannot be satisfied simultaneously have attracted widespread interest because very rich physics can appear in these systems [1]. For instance, multi-step magnetization behaviors have been experimentally observed in quite a number of frustrated spin systems, such as triangular spin-chain system $Ca_3Co_2O_6$ [2, 3] and Shastry–Sutherland (S–S) magnets [4–7]. Various theoretical and experimental explorations have been devoted to these interesting phenomena [8–11]. So far, it is generally believed that the multi-step magnetization behaviors in $Ca_3Co_2O_6$ are caused by non-equilibrium magnetization dynamics [12, 13], while those in S–S magnets are far from well understood. We address such phenomena in S–S magnets in this work.

The S–S lattice as a frustrated quantum antiferromagnetic (AFM) model with an exact ground state was first introduced by Shastry and Sutherland in the 1980s [14]. The lattice can be described as a square lattice with AFM couplings J' between the nearest neighbors and additional AFM couplings J between the next-nearest neighbors in every second square, as clearly shown in figure 1. As early as 1991, $SrCu_2(BO_3)_2$ with Cu^{2+} ions carrying a quantum spin $S = 1/2$ and located in a two-dimensional (2d) S–S lattice was investigated [15], triggering an extensive exploration of quantum S–S magnets which exhibit a fascinating sequence of magnetization (M) plateaus at fractional values of the saturated magnetization (M_s) [16, 17]. On the other hand, quite a few rare-earth tetraborides RB_4 (R = Tb, Dy, Ho, Tm, etc) with the magnetic moments located on a lattice that is topologically equivalent to the S–S lattice have attracted various interests [6, 7, 18, 19]. Similar to $SrCu_2(BO_3)_2$, complex magnetic structures and associated physical phenomena in these RB_4 compounds in response to magnetic field (h) at low temperature (T) were identified. In particular, magnetization multi-plateaus at the fractional values of M_s such as $M/M_s = 1/2, 1/7, 1/9$, etc, were observed in TmB_4 [7].

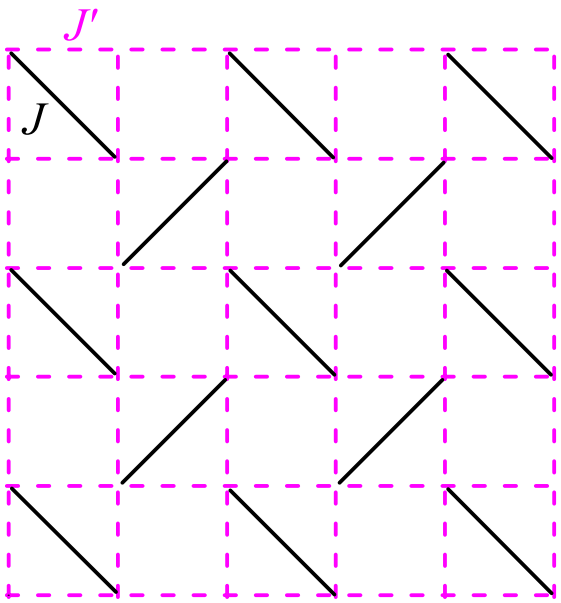

Figure 1. The Shastry–Sutherland lattice. J' bonds (dashed lines) are the exchange couplings along the edges of the squares and J bonds (solid lines) are the diagonal dimer couplings.

While a comprehensive understanding of the multi-step magnetization in $SrCu_2(BO_3)_2$ as a quantum magnet becomes challenging, TmB_4 presents a large total magnetic moment (the magnetic moment of Tm^{3+} is $\sim$6.0 μ_B), and thus can be considered as a classical spin system, making a theoretical approach easier. In addition, subjected to strong crystal field effects, TmB_4 exhibits strong easy-axis anisotropy and can be reasonably described by the classical Ising model rather than the Heisenberg one. Based on this fact, Cheng and Yang studied the magnetization process of the classical AFM Ising model on the S–S lattice using the tensor renormalization-group approach [20]. For a certain T range and coupling constants, only a single magnetization plateau at $M/M_s = 1/3$ resulting from a particular spin state in which each triangle contains two up-spins and one down-spin (UUD, see figure 2(a)) was predicted. Moreover, the spin-1/2 Ising-like XXZ model on the S–S lattice was also visited using the quantum Monte Carlo method, and the magnetization plateau at $M/M_s = 1/2$ was identified [21–23]. It was argued that quantum fluctuations and long-range interactions which may be considered to be the Ruderman–Kittel–Kasuya–Yosida (RKKY) interactions play an important role in the emergence of the $M/M_s = 1/2$ plateau, and a ferrimagnetic (FI) ground-state spin arrangement consisting of alternating AFM and ferromagnetic (FM) stripes was recognized, as depicted in figure 2(b). In addition, a model based on the coexistence of spin and electron subsystems was investigated to describe the magnetization processes in RB_4, and magnetization plateaus at $M/M_s = 1/2, 1/3, 1/5$, and $1/7$ were found [24]. It is

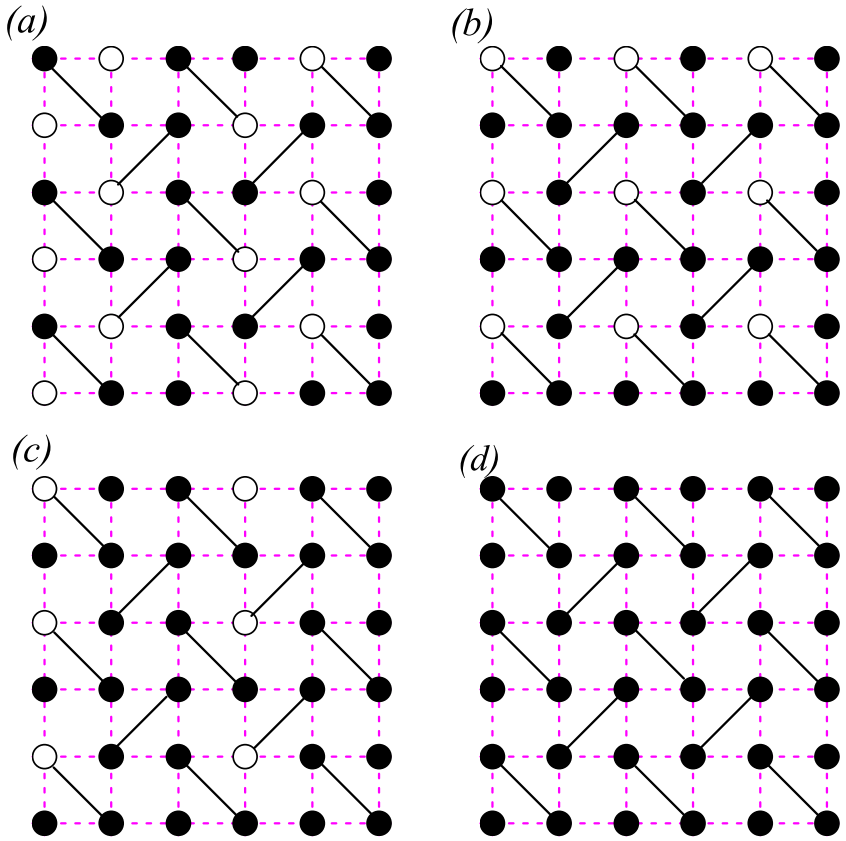

Figure 2. Spin configurations in the (a) UUD state, (b) FI state, (c) possible 2/3 plateau state, and (d) FM state. Solid and empty circles represent the up-spins and the down-spins, respectively.

believed that the interaction between the electron and spin subsystems may be responsible for the plateaus. This hints the substantial role of long-range interactions in determining the magnetization behaviors in these systems.

So far a complete understanding of the multi-step magnetization in TmB_4 remains open [25, 26]. For example, arguments concerning the origin of the experimentally observed 1/2 plateau in the high-h range have not yet reached an agreement. To some extent, an effective reduction of the neighboring spin interactions due to the spin frustration may enhance the relative importance of weak interactions. Besides the RKKY interaction, one such interaction is the long-range dipole–dipole (D–D) interaction, which is estimated to be on the same order of magnitude as the exchange coupling for rare-earth cations with considerable magnetic moments [27, 28]. When the D–D interaction is taken into account, spins in the system tend to be anti-parallel with each other, as will be stated later. Compared with the FM state (spin configuration is shown in figure 2(d)), the FI state with the plateau at $M/M_s = 1/2$ may be stabilized by the D–D interaction in a certain h region. In addition, a possible spin configuration with every AFM band separated by two FM stripes (figure 2(c)) may be stable when h is further increased, resulting in a magnetization plateau at $M/M_s = 2/3$.

Based on the above discussion on the possible spin configurations for the 1/2 and 2/3 magnetization plateaus, one may argue that the D–D interaction in the S–S magnets plays an important role in modulating the spin configuration. However, so far no work on this role of the D–D interaction has been available. In order to clarify this issue, we start with a classical Ising model on the 2d S–S lattice by including the D–D interaction, and then extensive simulations on the magnetization behavior are performed. The 1/2 plateau is indeed reproducible by including the D–D interaction, and the region for the FI state ($M/M_s = 1/2$) in the phase diagram can be significantly enlarged. Furthermore, the D–D interaction can also lead to a relatively narrow 2/3 plateau at low T.

2. Model and method

In the presence of a finite h, the Hamiltonian can be written as:

$$H = J' \sum_{\text{edges}} S_i \cdot S_j + J \sum_{\text{diagnol}} S_i \cdot S_j + g \sum_{\langle i,j \rangle} \left[\frac{S_i \cdot S_j}{\left| R_{ij}^3 \right|} - 3 \frac{\left(S_i \cdot R_{ij}\right)\left(S_j \cdot R_{ij}\right)}{\left| R_{ij}^5 \right|} \right] - h \sum_i S_i, \tag{1}$$

where the spin-exchange coupling $J' = 1/2, J = 1$, S_i is the Ising spin with unit length on site i, g is the dipolar factor, R_{ij} is the separation between sites i and j, and h is applied along the direction of up-spins ($+c$ axis). Since each Ising spin is along the c-axis, the second term in the D–D interaction can be safely ignored. In addition, a cut-off radius $R_{ij} = 6$ is chosen to save the CPU time, and it will be checked later that the choice of R_{ij} never affects our conclusion.

Our simulation is performed on an $L \times L$ (unless stated elsewhere, $L = 24$ is chosen) lattice with periodic boundary conditions using the standard Metropolis algorithm and the parallel tempering algorithm [29, 30]. Here, the parallel tempering algorithm is utilized in order to prevent the system from trapping in metastable free-energy minima caused by the frustration. We take an exchange sampling after every 10 standard Monte Carlo steps. Typically, the initial 2×10^4 Monte Carlo steps are discarded for equilibrium considerations and another 2×10^4 Monte Carlo steps are retained for statistic averaging of the simulation.

3. Simulation results and discussion

Figure 3(a) shows the calculated M as a function of g and h at $T = 0.02$. The magnetization curve for $g = 0$ clearly shows two steps. When h increases from zero, M rapidly reaches the first plateau at $M = M_s/3$ resulting from the UUD state, and then switches to M_s above $h \sim 3$. When g increases ($0 < g < 0.08$), a magnetization step at $M = 0$ is exhibited and gradually broadened. This plateau at $M = 0$ is caused by the collinear state (figure 3(c)), which is the same as the earlier report [20]. At the same time, the transition from the UUD state to the FM state shifts toward the high-h side, leading to the invariance of the plateau width at $M = M_s/3$ for $g < 0.08$. More interestingly, when g increases up to 0.08, a magnetization step at $M = M_s/2$ with the FI state is observed at a high-h range, which is consistent with experimental observation [7]. When g is further increased, the magnetization steps at $M = 0$ and $M = M_s/2$ are gradually broadened, while the step at $M = M_s/3$ is narrowed.

Figure 3(b) shows the simulated phase diagram in the g–h plane at $T = 0.02$, in which the transition points are estimated from the positions of the peaks in the susceptibility $\chi = \mathrm{d}M/\mathrm{d}h$, following earlier work [25]. In order to uncover the physics underlying our simulation, one may give a qualitative discussion from the energy landscape. At $g = 0$, the UUD state is stabilized by the magnetic energy when h is applied. As h further increases, the down-spins may flip as the static magnetic energy increases to be comparable with the interaction energy. The critical field can be estimated to be $h = 4J' + J = 3$, which is verified in our simulation. As stated earlier, spins in the system tend to be anti-parallel with each other when the D–D interaction is taken into account. Compared with the UUD state, the collinear state is stabilized by the D–D interaction. Thus, a higher h should be applied to convert the system from the collinear state to the UUD state as g increases, leading to the broadening of the magnetization step at $M = 0$. A similar behavior in the phase transition from the UUD state to the FM state can also be noticed, i.e. the transition shifts toward the high-h side as g increases ($0 < g < 0.08$), as clearly shown in figure 3(b). However, in the small g region ($g < 0.08$), the magnetic energy plays a significant role in modulating the step-M behavior, and the intermediate magnetization step at $M = M_s/2$ cannot be stabilized. On the other hand, in the large-g region ($g > 0.08$) in which the D–D interaction becomes more dominant, the magnetization

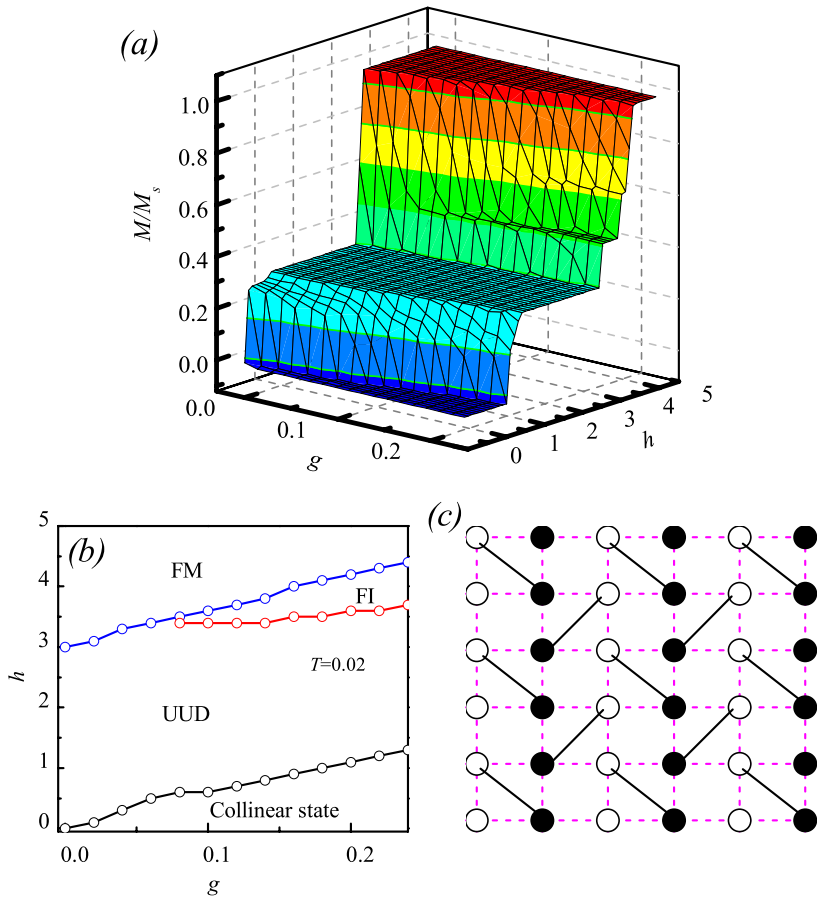

Figure 3. (a) Magnetization M versus dipolar factor g and magnetic field h. The parameters are $L = 24$, $T = 0.02$ and $R_{ij} = 6$. (b) Phase diagram of the magnetization plateau in the h–g plane. (c) Spin configuration for the collinear state with the plateau at $M = 0$. Solid and empty circles represent the up-spins and the down-spins, respectively.

step at $M = M_s/2$ is observed and is gradually enlarged with increasing g.

To identify the origin of the FI state with the 1/2 plateau, we respectively calculate the h-dependence of spin-exchange energy H_{ex}, D–D interaction H_{DD}, Zeeman energy H_{zee}, and the total energy H at $T = 0.02$ for $g = 0.2$ (see figure 4(a)). In order to help one to understand the results, the corresponding magnetization curve is also shown in figure 4(b). The enhancement of the FI state with increasing g may be understood from two different aspects. On one hand, within a certain h range, the energy loss from the D–D interaction and spin-exchange interaction due to the phase transition from the UUD state to the FI state is smaller than the energy gain from the Zeeman energy, leading to the stabilization of the FI state. In addition, the energy loss from the D–D interaction due to this transition is very small and increases slowly with increasing g, thus the transition from the UUD state to the FI state occurs at a relatively stable h, as shown with the red circles in figure 3(b). On the other hand, the energy loss from the D–D interaction due to the phase transition from the FI state to the FM state is large and increases quickly as g increases. So, a larger h will be needed to flip down-spins in the FI state with increasing g. As a result, when g is further increased from $g = 0.08$, the region of the FI state with the plateau at $M = M_s/2$ is enlarged, while that of the FM state with the plateau at $M = M_s$ is narrowed.

In addition, the effect of T is also studied in our simulation, and the corresponding results are shown in figure 5. Figure 5(a) shows the calculated M as a function of T and h for $g = 0.2$. At low T ($T < 0.02$), a narrow magnetization plateau at $M = 2M_s/3$ is observed in addition to the previously discussed plateaus at $M = 0, M_s/3, M_s/2$ and M_s. The spin configuration with the plateau at $M = 2M_s/3$ is confirmed in our work to be the same as that shown in figure 2(c). The related physical mechanism responsible for this phenomenon may be similar to that for the emergence of the plateau at $M = M_s/2$ in a certain h range. However, the $2M_s/3$ plateau is so unstable that it quickly disappears when T increases slightly, as shown in figure 5(b). In addition, the FI state is gradually destroyed due to the thermal fluctuations, leading to the melting of the magnetization step at $M = M_s/2$. When T is raised to about 0.15, the $M_s/2$ plateau completely disappears. On the other hand, the steps at $M = 0$ and $M_s/3$ are relatively stable, and are clearly visible even at $T = 0.4$. However, when T rises from 0.15, the borders between the steps become more and more indistinct, as shown in figure 5(a). One may note that the perfect collinear state and UUD state may be partially destroyed near the critical

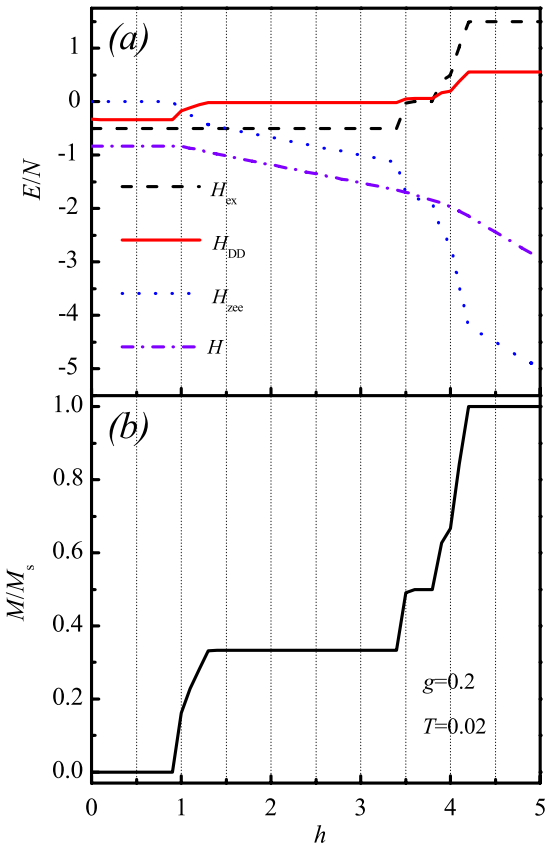

Figure 4. The calculated (a) H_{ex}, H_{DD}, H_{zee}, H, and (b) magnetization M/M_s as a function of h at $T = 0.02$ for $g = 0.2$.

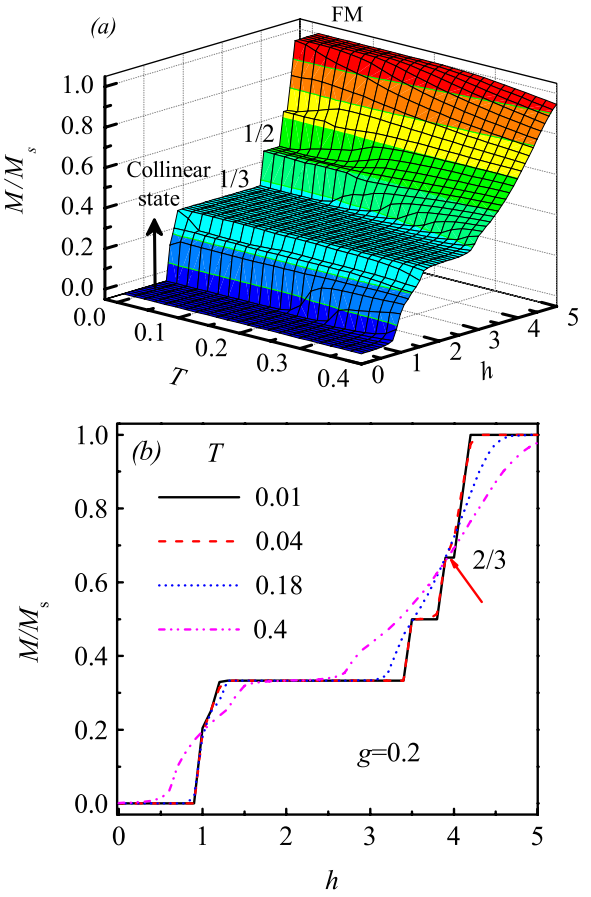

Figure 5. (a) Magnetization M/M_s versus temperature T and magnetic field h for $g = 0.2$. (b) Magnetization curves for different T for $g = 0.2$.

field at high T ($T > 0.15$), leading to the smoothness of the magnetization curves.

Up to now, the present work reveals that frustrated spin systems such as TmB_4 offer a very complicated spin configuration which is very sensitive to weak interactions, including the D–D interaction which is usually ignored in earlier work. The magnetization plateau at $M = M_s/2$ at low T as reported in experiments is reproduced in our simulation when the D–D interaction is taken into account. In addition, a narrow step at $M = 2M_s/3$ is predicted in our simulation, which remains to be checked further. Although not all the experimental results in TmB_4 can be explained based on the classical Ising model, the present study has taken an important step toward a complete understanding of the magnetization process of this system.

In order to verify the reliability of our simulation, the dependence of the step-like magnetization feature on the cut-off radius R_{ij} and the lattice size L has also been investigated, and the simulated results are presented in figure 6. Figure 6(a) shows the simulated magnetization curves for various R_{ij} ($R_{ij} = 4$, 6 and 8) at $T = 0.02$ for $g = 0.2$. The magnetization curve for $R_{ij} = 6$ perfectly coincides with that for $R_{ij} = 8$, indicating that the choice of R_{ij} in this work is reasonable enough. Finally, we check the finite-lattice-size effect in order to exclude the artificial facts due to the finite lattice size in our simulation. The simulated magnetization curves for different L ($L = 12$, 18, 24 and 30) are shown in figure 6(b). The simulated curves for various L are almost merged into one, demonstrating that the finite-size effect on the magnetization of the system is negligible and never affects our conclusion.

4. Conclusion

In conclusion, we have studied the magnetic behavior of the classical Ising model on the Shastry–Sutherland lattice by means of Monte Carlo simulation in order to understand the magnetic process in TmB_4. Our simulation successfully reproduces the magnetization plateau at $M = M_s/2$ observed in experiments when the D–D interaction is taken into account. In addition, a tiny plateau at $M = 2M_s/3$ is predicted in our work, which deserves to be checked further. The magnetic phase diagram can be understood from the competitions among the spin-exchange interaction, the D–D interaction and the static magnetic energy. It is indicated that even weak interactions available in realistic systems, such as the D–D interaction, may have a significant effect on the step-like magnetization feature. The present work may provide new insights into the understanding of the magnetization process for frustrated S–S magnets.

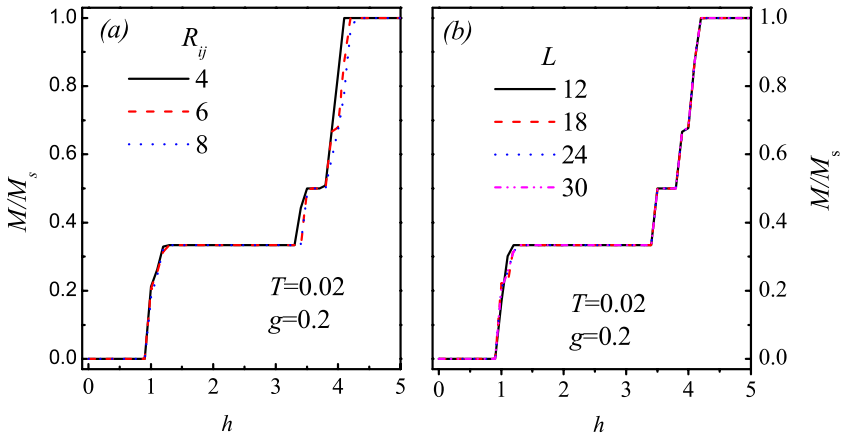

Figure 6. Magnetization curves for (a) different cut-off radius R_{ij} and (b) different lattice sizes L. The parameters are $T = 0.02$ and $g = 0.2$.

Acknowledgments

This work was supported by the National Key Projects for Basic Research of China (2011CB922101), the Natural Science Foundation of China (11204091, 11274094, 50832002, 51031004), China Postdoctoral Science Foundation funded project (20100480768), and the Priority Academic Program Development of Jiangsu Higher Education Institutions, China.

References

[1] Diep H T 2004 *Frustrated Spin Systems* (Singapore: World Scientific)
[2] Kageyama H, Yoshimura K, Kosuge K, Azuma M, Takano M, Mitamura H and Goto T 1997 *J. Phys. Soc. Japan* **66** 3996
[3] Maignan A, Michel C, Masset A C, Martin C and Raveau B 2000 *Eur. Phys. J.* B **15** 657
[4] Kageyama H, Yoshimura K, Stern R, Mushnikov N V, Onizuka K, Kato M, Kosuge K, Slichter C P, Goto T and Ueda Y 1999 *Phys. Rev. Lett.* **82** 3168
[5] Kodama K, Takigawa M, Horvatic M, Berthier C, Kageyama H, Ueda Y, Miyahara S, Becca F and Mila F 2002 *Science* **298** 395
[6] Yoshii S, Yamamoto T, Hagiwara M, Michimura S, Shigekawa A, Iga F, Takabatake T and Kindo K 2008 *Phys. Rev. Lett.* **101** 087202
[7] Siemensmeyer K, Wulf E, Mikeska H J, Flachbart K, Gabani S, Matas S, Priputen P, Efdokimova A and Shitsevalova N 2008 *Phys. Rev. Lett.* **101** 177201
[8] Kudasov Y B 2006 *Phys. Rev. Lett.* **96** 027212
[9] Yao X Y, Dong S and Liu J-M 2006 *Phys. Rev.* B **73** 212415
[10] Abendschein A and Capponi S 2008 *Phys. Rev. Lett.* **101** 227201
[11] Dorier J, Schmidt K P and Mila F 2008 *Phys. Rev. Lett.* **101** 250402
[12] Qin M H, Wang K F and Liu J-M 2009 *Phys. Rev.* B **79** 172405
[13] Kudasov Y B, Korshunov A S, Pavlov V N and Maslov D A 2008 *Phys. Rev.* B **78** 132407
[14] Shastry B S and Sutherland B 1981 *Physica* B + C **108** 1069
[15] Smith R W and Keszler D A 1991 *J. Solid State Chem.* **93** 430
[16] Alicea J, Chubukov A V and Starykh O A 2009 *Phys. Rev. Lett.* **102** 137201
[17] Isaev L, Ortiz G and Dukelsky J 2009 *Phys. Rev. Lett.* **103** 177201
[18] Watanuki R, Sato G, Suzuki K, Ishihara M, Yanagisawa T, Nemoto Y and Goto T 2005 *J. Phys. Soc. Japan* **74** 2169
[19] Michimura S, Shigekawa A, Iga F, Swra M, Takabatake T, Ohoyama K and Okabe Y 2006 *Physica* B **378** 596
[20] Chang M C and Yang M F 2009 *Phys. Rev.* B **79** 104411
[21] Meng Z Y and Wessel S 2008 *Phys. Rev.* B **78** 224416
[22] Suzuki T, Tomita Y and Kawashima N 2009 *Phys. Rev.* B **80** 180405
[23] Suzuki T, Tomita Y and Kawashima N 2010 *Phys. Rev.* B **82** 214404
[24] Farkasovsky P, Cencarikova H and Matas S 2010 *Phys. Rev.* B **82** 054409
[25] Moliner M, Cabra D C, Honecker A, Pujol P and Stauffer F 2009 *Phys. Rev.* B **79** 144401
[26] Qin M H, Zhang G Q, Wang K F, Gao X S and Liu J-M 2011 *J. Appl. Phys.* **109** 07E103
[27] Melko R G, Hertog B C and Gingras M J P 2001 *Phys. Rev. Lett.* **87** 067203
[28] Xie Y L, Lin L, Yan Z B, Wang K F and Liu J-M 2012 *J. Appl. Phys.* **111** 07E133
[29] Landau D P and Binder K 2008 *A Guide to Monte Carlo Simulations in Statistical Physics* (Cambridge: Cambridge University Press)
[30] Hukushima K and Nemoto K 1996 *J. Phys. Soc. Japan* **65** 1604